International Journal of Robotics and Control Systems
Vol. 5, No. 2, 2025, pp. 781-793
ISSN 2775-2658
http://pubs2.ascee.org/index.php/ijrcs

Four DOF Robot Manipulator Control Using Feedback Linearization Based on Sliding Mode Control

Walid Kh. Alqaisi [a,1], Mostafa Soliman [a,2,*], Ahmed Badawi [a,2,*], I.M. Elzein [a,3], Claude Ziad El-Bayeh [b,4]

[a] College of Engineering and Technology, University of Doha for Science and Technology, 24449 Arab League St, Doha, Qatar
[b] Canada Excellence Research Chair Team, Concordia University, Montreal, Canada
[1] walid.alqaisi@udst.edu.qa; [2] mostafa.soliman@udst.edu.qa; [3] ahmedbadawi100@gmail.com;
[4] 4360101973@udst.edu.qa; [5] c.bayeh@hotmail.com
* Corresponding Author

ARTICLE INFO

Article history
Received December 04, 2024
Revised January 11, 2025
Accepted February 15, 2025

Keywords
Robot Arm;
Manipulator;
4DOF Robot;
Feedback Linearization;
Sliding Mode Control

ABSTRACT

This paper investigates the performance of a four-degree-of-freedom (4DOF) robot arm using feedback linearization based on sliding mode control (FLSM). FLSM simplifies complex nonlinear control solutions and mitigates the effects of the highly coupled dynamic behavior of the 4DOF manipulator. The controller takes into account uncertain dynamics and unexpected disturbances such as changes in payload, variations in wind, and gravity effects in different directions. The stability of the proposed controller is achieved using the manipulator model and FLSM without linearizing the model. Stability is analyzed using a Lyapunov function, and MATLAB Simulink is utilized to simulate the real parameters of the Quanser QArm. The results are compared with those obtained using a PID controller.

1. Introduction

In recent decades, robotics control methodologies for nonlinear mechanical systems have garnered significant attention from researchers [1]. An important example is a robot manipulator arm, which poses a challenge due to its highly nonlinear nature and coupled dynamics. The additional degrees of freedom enhance flexibility and resolution, allowing a wider range of tasks to be performed. In the industrial manufacturing sector, there is an increasing preference for multi-axis robots, such as 4-DOF configurations. This trend is particularly significant in processes like laser tracking and industrial welding, where increased flexibility can lead to improved processing precision [2]. However, the complexity of dynamics associated with higher DOFs in multi-axis robots poses challenges for accurate trajectory tracking. Furthermore, operations involving high payloads may intensify these challenges, resulting in considerable disturbances. Therefore, the implementation of a robust controller is crucial for effective tracking in multi-axis robotic systems. This research focuses on the development of a controller for a 4-DOF robot manipulator [3], In academic literature, numerous approaches have been proposed to manage manipulator robots. Friction in joints is addressed by using a robust control method to control a two-degree-of-freedom manipulator robot [4], [5]. An adaptive control structure was implemented in [6] to mitigate the adverse effects of unidentified nonlinearities. An optimal control of a linearized feedback is used in [7], [8]. A fast

predictive control for a high speed robot arm is used in [9]. A feedforward neural network was constructed to solve the problematic inverse kinematics of a robotic planar manipulator with three degrees of freedom [10], where the accuracy of trajectory generation in Cartesian space is crucial for controlling the robot arm. Backstepping control is used with disturbance and uncertainty estimation using a neural network is used in [11]. Hierarchical ML for a manipulator is used in [12]. Reference [13] proposed a hybrid control method for a three-link robotic arm consisting of joint control designed in space configuration and sliding mode control. Reference [14] suggests a time-optimal trajectory for a robotic system using a convex optimization approach. An adaptive control system was developed for a robotic arm in [15], incorporating linear quadratic techniques to enhance performance. An optimal adaptive sliding mode was implemented and tested with a disturbance observer on a robot arm in [16]. Observability analysis is used to drive linearized feedback is used in [17]. Three methods of nonlinear predictive control were developed in [18] to supervise two interconnected vertical manipulator robots. An adaptive radial-based controller was used in [19]. Reference [20] recommended anticipating a robotic manipulator of a nonlinear model mounted on an autonomous platform. Feedback linearization for a quadrotor was successfully implemented in [21]. Multivariable super-twisting control was introduced to tackle uncertainties in [22] and [23]. A hierarchical perturbation controller was introduced in [24].

Reference [25] used a modified PD control law with Taylor-series compensation to achieve robust reference tracking. Conversely, conventional feedback linearization controllers are designed to ensure that the system converges asymptotically to zero. The work cited in [26] presents an innovative adaptive continuous sliding mode strategy designed to tackle uncertainties and alleviate the chattering phenomena often encountered during control operations. References [27] and [28] explore a nonsingular fast terminal second-order sliding mode methodology for robotic manipulators based on feedback linearization principles. Furthermore, a hierarchical perturbation compensation system incorporating an exponential reaching law sliding mode controller is examined in the quadrotor framework in [29].

SMC has become a prominent control technology, recognized for its simplicity and effectiveness in handling uncertainties and disturbances. The stability and stabilization aspects of SMC are fundamentally anchored in the principles of Lyapunov theory, providing a framework for establishing asymptotic stability. SMC is specifically engineered to maintain robust control performance in the presence of confined disturbances and uncertainties. It has become a fundamental technique to address parametric uncertainties inherent in complex multi-input multi-output (MIMO) nonlinear systems. Conventional and high-order SMC is introduced in reference [30]. A design for a second-order sliding mode controller that incorporates output constraints is presented in reference [31]. Additionally, reference [32] discusses a novel adaptive sliding-mode control scheme specifically tailored for robot manipulators.

Driven by the benefits of both SMC and Feedback Linearization, a controller that combines these two approaches, termed Feedback Linearization based Sliding Mode Control (FLSM), has been developed based on extensive research. Feedback Linearization is employed as a nonlinear design technique to address the nonlinear dynamics of the mechanical system efficiently. The controller is structured in two loops: the inner loop addresses the significant nonlinearities of the robot arm parameters, while the outer loop integrates the robust aspects of the sliding mode controller to manage nonlinear uncertainties and disturbances. This method is resilient to variations in robot parameters, and the stability of the quadrotor system and the finite-time convergence of errors are validated using the Lyapunov function.

The performance improvement of a Feedback Linearization Sliding Mode (FLSM) controller over a PID controller can be seen in many aspects, FLSM controllers handle system nonlinearities and uncertainties better than PID controllers, which rely on linear assumptions and tuning. FLSM can adapt dynamically to changing conditions, resulting in lower overshoot and minimal oscillations compared to PID. The sliding mode aspect of FLSM ensures robust tracking and stability, even in the presence of external disturbances and modeling errors. FLSM achieves quicker convergence to the

desired setpoint with faster error correction, compared to PID's proportional, integral, and derivative adjustments. FLSM excels in managing complex, time-varying, or highly coupled systems where PID may struggle due to its simplicity [33]. The key contributions of this paper are outlined as follows:

- Introducing a control system that effectively addresses nonlinearity without resorting to model linearization, utilizing feedback linearization principles and adaptive SMC methodologies.
- Mitigating the impact of severe nonlinearity and tightly coupled dynamics, ensuring robust and precise control.
- Applying the system to the QArm, a four-degree-of-freedom system, in an aggressive trajectory with disturbances.

2. Dynamic Model of the Robot Arm

The dynamic modeling of a robotic arm articulates the correlation between the forces and torques applied to the robot's joints and the resulting motion [34], [35]. This modeling involves analyzing the arm's physical attributes, such as mass, inertia, and friction, along with the kinematic and dynamic equations that govern its operation.

The dynamic model of a robotic arm serves as a mathematical framework that explains how the arm moves in response to applied forces and torques. It illustrates the interaction between the arm's physical characteristics and the forces acting on it, including joint torques, gravitational effects, and frictional forces. This model is essential for predicting the arm's behavior under different conditions and is crucial for developing control systems that ensure precise and efficient control of the robot's movements.

Analyzing the dynamics of robot manipulators presents significant challenges. Researchers have explored various techniques, primarily categorized into the Euler-Lagrange formulation and the Newton-Euler formulation. The Euler-Lagrange method views the manipulator as a unified system, focusing on its kinetic and potential energy for analysis. In contrast, the Newton-Euler approach treats each link of the manipulator individually, starting with forward recursion to describe linear and angular motions, followed by backward recursion to evaluate forces and torques.

The comparison of efficiency between the Euler-Lagrange and Newton-Euler formulations remains a prominent topic in the field [36]. The choice of method depends on factors such as the number of links and joints in the kinematic chain, the chain's topology, the orientation of coordinate frames, and the use of recursive procedures [37]. Generally, the Newton-Euler formulation is preferred for manipulators with many degrees of freedom due to its recursive nature, especially when frames are appropriately configured.

To obtain accurate dynamic parameters, identification techniques leveraging the nonlinearity of the dynamic model can be employed. The Quanser robot arm manipulator is frequently discussed in research papers, and maintaining frame assignments is crucial for accurate modeling.

In this section, we will demonstrate the modeling of the Quanser four-degree-of-freedom (DOF) QArm manipulator. The kinematic diagram in Fig. 1 illustrates the x and z axes of each joint frame, while the rigid body diagram provides the x, y, or z axes for notation convenience. The third axis can be determined using the right-hand rule. The dynamic equations can be represented in matrix form as [29], [38]:

$$\tau = M(\theta)\ddot{\theta} + B\,(\theta)\dot{\theta}_i\dot{\theta}_j + C\,(\theta)\dot{\theta}_k^2 + G(\theta) \quad (1)$$

Where, $(i,\ j)\epsilon\ \{(1,2),(1,3),(1,4),(2,3),(2,4),(3,4)\}$,

$k\epsilon\ \{1,2,3,4\}$, In this context, (M=Inertia matrix), ($\boldsymbol{B}$=Coriolis matrix), ($\boldsymbol{C}$= signifies the Centrifugal matrix), and ($\boldsymbol{G}$=Gravity matrix). This representation, referred to as an equation of motion. It, illustrates that the matrices corresponding to the Coriolis and Centrifugal coefficients are solely

dependent on the manipulator's state ϕ. It is important to note that certain coefficients within these matrices may be rendered inapplicable or equal to zero, contingent upon the specific configuration of the manipulator. For the Quanser Arm, these matrices are structured in a particular manner.

$$\begin{bmatrix}\tau_1\\ \tau_2\\ \tau_3\\ \tau_4\end{bmatrix}=\begin{bmatrix}M_{11} & 0 & 0 & M_{14}\\ 0 & M_{22} & M_{23} & 0\\ 0 & M_{32} & M_{33} & 0\\ M_{41} & 0 & 0 & M_{44}\end{bmatrix}\begin{bmatrix}\ddot{\theta}_1\\ \ddot{\theta}_2\\ \ddot{\theta}_3\\ \ddot{\theta}_4\end{bmatrix}+\begin{bmatrix}B_{11} & B_{12} & 0 & 0 & B_{15} & B_{16}\\ 0 & 0 & B_{23} & B_{24} & 0 & 0\\ 0 & 0 & B_{33} & 0 & 0 & 0\\ B_{41} & B_{42} & 0 & 0 & 0 & 0\end{bmatrix}\begin{bmatrix}\dot{\theta}_1\dot{\theta}_2\\ \dot{\theta}_1\dot{\theta}_3\\ \dot{\theta}_1\dot{\theta}_4\\ \dot{\theta}_2\dot{\theta}_3\\ \dot{\theta}_2\dot{\theta}_4\\ \dot{\theta}_3\dot{\theta}_4\end{bmatrix}+\begin{bmatrix}0 & 0 & 0 & 0\\ C_{21} & 0 & C_{23} & 0\\ C_{31} & C_{32} & 0 & 0\\ 0 & 0 & 0 & 0\end{bmatrix}\begin{bmatrix}\dot{\theta}_1^2\\ \dot{\theta}_2^2\\ \dot{\theta}_3^2\\ \dot{\theta}_4^2\end{bmatrix}+g\begin{bmatrix}0\\ G_2\\ G_3\\ G_4\end{bmatrix} \quad (2)$$

Coefficients denoted by the subscript mn signify the relationship between the torque exerted at the m^{th} joint and the associated n^{th} kinematic term. For instance, the B_{24} coefficient connects the torque on joint 2, represented as $\tau 2$, to the corresponding fourth kinematic term, which is expressed as, $\dot{\theta}_2\dot{\theta}_3$. According to Fig. 1, the manipulator is currently at the home stage positioning. The joint space vector θ can be represented as, $\theta = [0, (\beta - \frac{\pi}{4}), -\beta, 0]^T$.

Both the actuators and encoders of the manipulator are fully calibrated at this position. To move the manipulator to the home position, a $[0\ 0\ 0]^{\text{T}}$ command must be applied. Additionally, the encoder will also read the joint position as $[0\ 0\ 0]^{\text{T}}$. The joint space alternation may be represented as $\vec{\phi}$. Further description of the manipulator $\vec{\phi}$ space is addressed in Table 1. For example, when $\phi 2=0$ it will convey $\theta 2=\beta-\pi/2$. This pertains to joint 2 from the perspective of home position. Further description of the robot arm model are detailed in [38]. Dynamic parameters for the Qarm shown in Table 2.

Table 1. simplification of mathematical formulation through linear mapping

New Parameter	Original Parameter	New Parameter	Original Parameter
λ_1	L_1	$\emptyset_1$	θ_1
λ_2	$\sqrt{L_2^2 + L_3^2}$	$\emptyset_2$	$\theta_2 + \frac{\pi}{2} - \beta$
λ_3	$L_4 + L_5$	$\emptyset_3$	$\theta_3 + \beta$
β	$\tan^{-1}(\frac{L_3}{L_2})$	$\emptyset_4$	θ_4

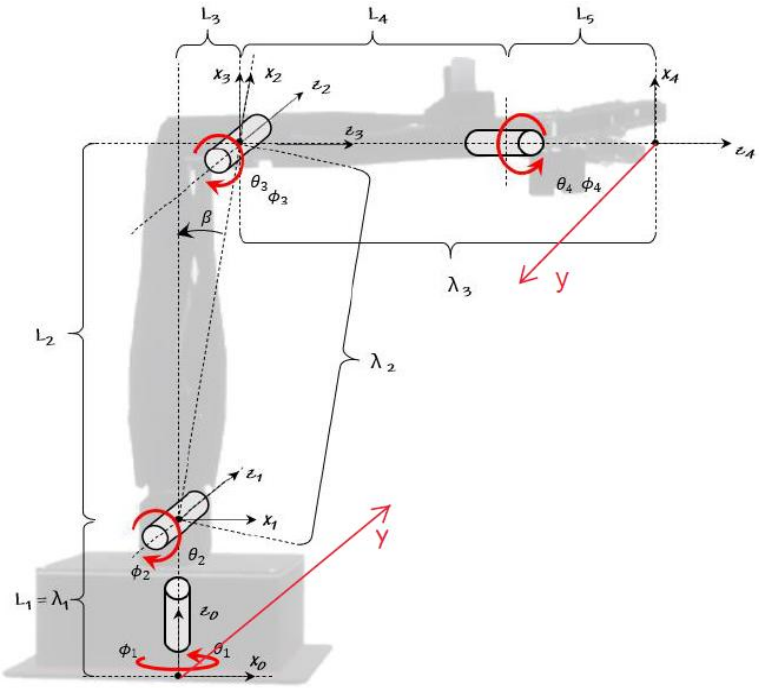

Fig. 1. Frame diagram of Quanser Arm manipulator [38]

Table 2. Dynamic parameters for the Qarm

Parameter	Value	Parameter	Value
m_1	0.7906 kg	m_2	0.4591 kg
λ_{c1}	0.0399 m	λ_{c2}	0.1071 m
I_{1A}	1.489 × 10^{-3} kg m^2	I_{2A}	1.922 × 10^{-4} kg m^2
n/a^*	-	$I_{2L}{}^*$	1.610 × 10^{-3} kg m^2
Parameter	**Value**	**Parameter**	**Value**
m_3	0.269 kg	m_4	0.257 kg
λ_{c3}	0.1561 m	λ_{c4}	0.0998 m
I_{3A}	2.679 × 10^{-4} kg m^2	I_{4A}	6.528 × 10^{-4} kg m^2
$I_{3L}{}^*$	2.069 × 10^{-3} kg m^2	$I_{4L}{}^*$	1.120 × 10^{-3} kg m^2

3. Controller Design

The procedure for synthesizing the controller is designed to guarantee stability while enabling the quadrotor to adhere to a specified trajectory. Feedback linearization is a control strategy used to handle nonlinear systems by transforming them into an equivalent linear system through mathematical manipulation. This is achieved by designing a control law that cancels out the nonlinear dynamics of the system, leaving a linearized behavior that can be easily controlled using standard linear control techniques. It effectively simplifies the design and analysis of controllers for complex systems.

A Lyapunov function is a scalar mathematical function used to assess the stability of a dynamic system. It is analogous to an "energy-like" measure for the system, where the function decreases over time for a stable system, indicating that the system's state is converging to an equilibrium point. In engineering, Lyapunov's direct method leverages this function to prove stability without solving the system's differential equations explicitly, making it a powerful tool for nonlinear control design.

3.1. Control Algorithm

This section presents the implementation of a robust sliding mode controller that integrates a Feedback linearization approach. The objective of the proposed system is to achieve asymptotic convergence of the error while accommodating nonlinear uncertainties and external disturbances. The linearization process employs an input/output feedback linearization technique, which is executed through two distinct loops: the inner and outer loops. The inner loop is specifically designed to mitigate the impact of the system's hard nonlinearity, thereby establishing a relationship between input and output states and formulating a nonlinear control law. Conversely, the outer loop focuses on regulating the input/output system to ensure the stabilization of the closed-loop system and to facilitate the estimation of nonlinear uncertainties. The control system's block diagram is illustrated in Fig. 2. The primary aim of the input-output system is to establish a direct correlation between the system's output and its input control action. According to equation (4), the desired input U can be expressed as follows:

$$\tau = M(\theta)v + B\ (\theta)\dot{\theta}_i\dot{\theta}_j + C\ (\theta)\dot{\theta}_k^2 + G(\theta) \tag{3}$$

Knowing that, v is a supplementary controlling input to the model and v= $[v_1\ ,\ v_2\ ,\ v_3\ ,\ v_4]^T$. According to (3), a clear and direct relationship between the control input and the system's output exists, allowing the system to be restructured to emphasize this linkage [39] and [40]:

$$\ddot{\theta}=v+D(t) \tag{4}$$

Where; $D(t)$ = bounded uncertainty.

Assumption*:* we assume the term of uncertainties, is globally Lipchitz function.

The desired trajectory θ_d is obtained from the required robot mission. $E=\theta-\theta_d\ \epsilon R^n$ and $\dot{E}=\dot{\theta}-\dot{\theta}_d\ \epsilon R^n$ represent the error along its derivation. The sliding variable along its derivation is designated as per the notations [39]:

$$S = \dot{E} + \Lambda E$$
$$\dot{S} = \ddot{E} + \Lambda \dot{E} \quad (5)$$

Where; $\Lambda = diag(\lambda_{ii})$ for $i = 1, \dots, to\ n$ is a diagonal positive definite matrix and (n) is the length of the states vector. The velocity and acceleration of the desired trajectory $\dot{\theta}_d, \ddot{\theta}_d$ are measurable quantities in the manipulator. The auxiliary input v is designed as described in Equation (6), [40]:

$$v = \ddot{\theta}_d - \Lambda \dot{E} - K\ SGN - D(t) \quad (6)$$

Where; $K = diag(k_{ii})$ for $i = 1, \dots, to\ n$ is a positive-definite diagonal matrix. $SGN = [Sign(s_1),\ Sign(s_2),\ Sign(s_3),\ Sign(s_4)]^T$, and the function $Sign(s_i)$, is defined such that:

$$Sign(s_i) = \begin{cases} 1 & for\ s_i > 0 \\ 0 & for\ s_i = 0 \\ -1 & for\ s_i < 0 \end{cases} \quad (7)$$

Theorem:

In the context of the quadrotor system outlined in (1), the control inputs of 6, 4, and 3 facilitate the finite-time convergence of the sliding surface defined by S(x, t) = 0. Consequently, both the tracking error E and its derivative Ė will asymptotically approach zero.

Proof:

It is appropriate to identify the following Lyapunov function:

$$V = \frac{1}{2} S^T S \quad (8)$$

The time derivative of Lyapunov functions is specified by:

$$\dot{V} = S^T \dot{S} \quad (9)$$

By substituting the derivative of the selected surface as shown in equation (5), we derive the following result:

$$\dot{V} = S^T(\ddot{E} + \Lambda \dot{E}) = S^T[\ddot{\theta} - \ddot{\theta}_d + \Lambda \dot{E}] \quad (10)$$

Substituting equation (1) into equation (10) gives:

$$\dot{V} = S^T[M^{-1}(\theta)(\tau - B\ (\theta)\dot{\theta}_i\dot{\theta}_j - C(\theta)\dot{\theta}_k^2 - G(\theta)) - \ddot{\theta}_d + \Lambda \dot{E}] \quad (11)$$

By substituting the control inputs (3) and (6) into equation (11), we find:

$$\dot{V} = S^T[(-K\ SGN - D(t))]$$
$$\dot{V} = -\sum_{i=1}^{4} s_i\ (k_i\ sign(s_i) - D_i(t))$$
$$\leq -\sum_{i=1}^{4} |s_i|\ (|k_i\ sign(s_i)| - |D_i(t)|) \quad (12)$$
$$\leq -\sum_{i=1}^{4} |s_i|\ (k_i\ - |D_i(t)|)$$

To ensure that $\dot{V}$ is less than 0, the gain must be selected as $k_i > D_i$. Once this condition is met, the stability of the system is verified.

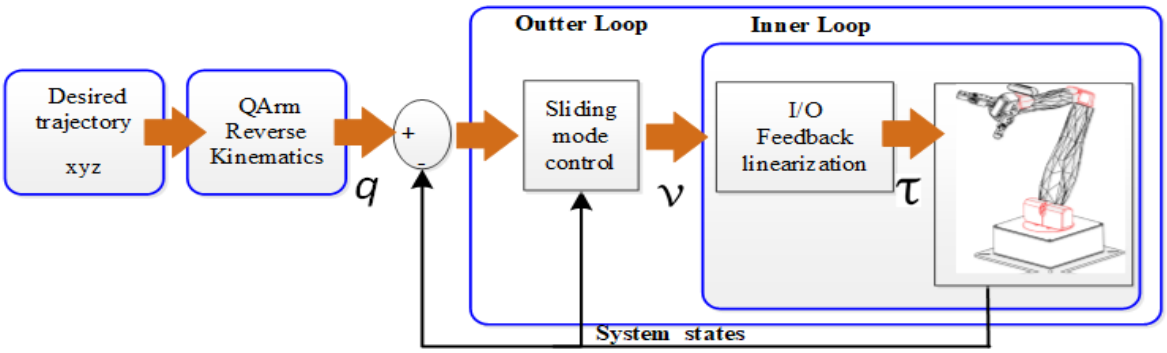

Fig. 2. Control system block diagram

4. Simulation Results

The simulation outcomes are based on the actual parameters of the Quanser Robot QArm, as shown in Fig. 3. The robot model in equations (1) and (2) is used, with M_{ij}, B_{ij}, and C_{ij} detailed in [38]. The QArm parameters are listed in Table 2. The initial values of the joints are $q_1 = q_2 = q_3 = q_4 = 0$, corresponding to $x = 45cm, y = 0\ cm$ and $z = 49\ cm$. To showcase the resilience of the proposed control schemes, a time-varying disturbance is introduced to the controlled signal. The external disturbances are assumed to be as follows:

$$D_i = 3\ cos(\omega t) + 0.5\ sin(\omega t) \tag{13}$$

The control feedback linearization based on sliding mode controller described in section 3 is used. The gain values are as follows:

$$\Lambda = diag[10,10,10,1000],$$

$$K = diag[100,100,100,500]$$

The desired trajectory consists of two squares with sharp edges, as shown in Fig. 4. The graph illustrates the performance of the trajectory tracking system. Fig. 5 and Fig. 6 depict the tracking of the three axes and the joint tracking, showcasing the controller's ability to provide precise tracking. Additionally, the proposed controller is compared to a standard PID controller.

$$\tau = K_p e(t) + K_D \frac{d}{dt} e(t) + K_I \int e(t)dt \tag{14}$$

The errors in the axes for the proposed controller, which is based on feedback linearization utilizing sliding mode, are presented in Fig. 7, along with the PID controllers. It is evident that the proposed control reduces the error. Fig. 8 displays the control signals, showing continuous signals that never reach saturation, indicating the capability to apply to a practical system to verify the controller's quality and stability. The controller regulates the behavior of a system to achieve desired performance. Control signals are smooth and uninterrupted over time, without abrupt jumps or discontinuities which reduces stress on the system's actuators and improves overall performance and indicates the controller operates within a safe range, avoiding potential issues like degraded performance or system instability. System stability ensures the system does not oscillate uncontrollably or deviate from the desired state.

The root mean square (RMSE) value of the errors in each case is shown in Table 3. The numbers in the table show the advantage of FLSMC over the PID controller. The proposed combined system provides good performance as shown in the figures and the table.

As it can be noticed in the simulation the FLSM controller over a PID controller has improved Robustness to Nonlinearities, Reduced Overshoot and Oscillations, Improved Stability, ensured Faster

Response, and Reduced Sensitivity to Tuning. The FLSM demonstrated superior robustness and precision under varying conditions compared to the PID controller, effectively maintaining stability and accuracy even in challenging scenarios.

Table 3. Root mean square of the errors

RMSE	PID	FLSM
x	0.3818	0.036
y	0.1377	0.03
z	0.03	0.002

Fig. 3. Quanser QArm [38]

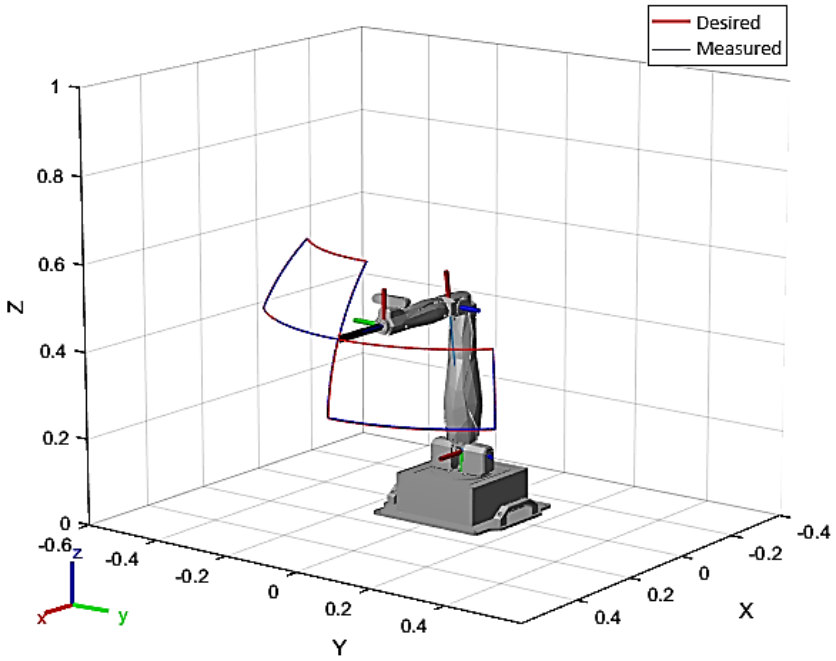

Fig. 4. Trajectory tracking in3D

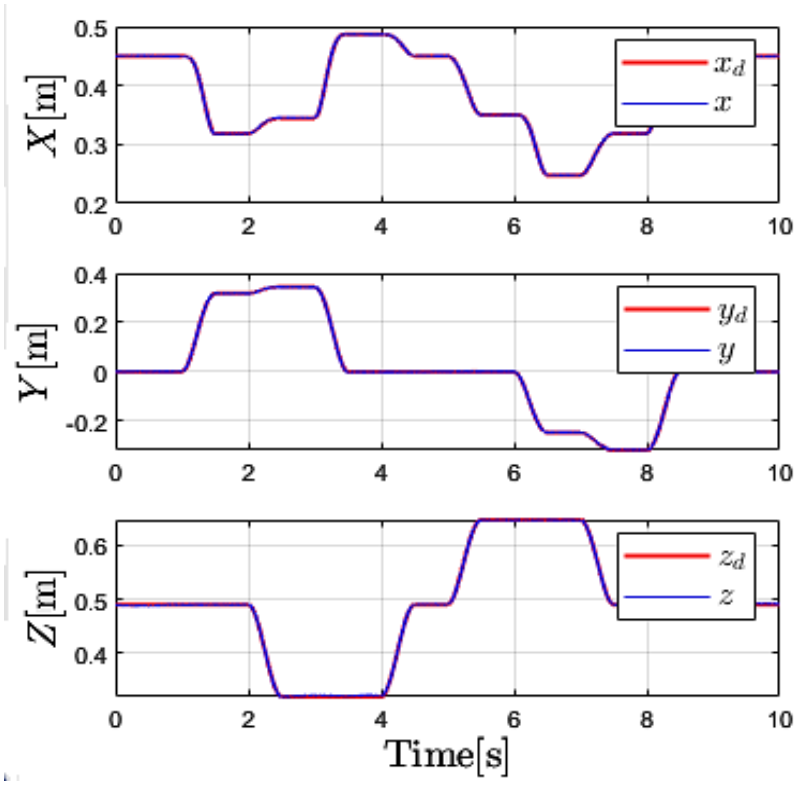

Fig. 5. Trajectory tracking in xyz

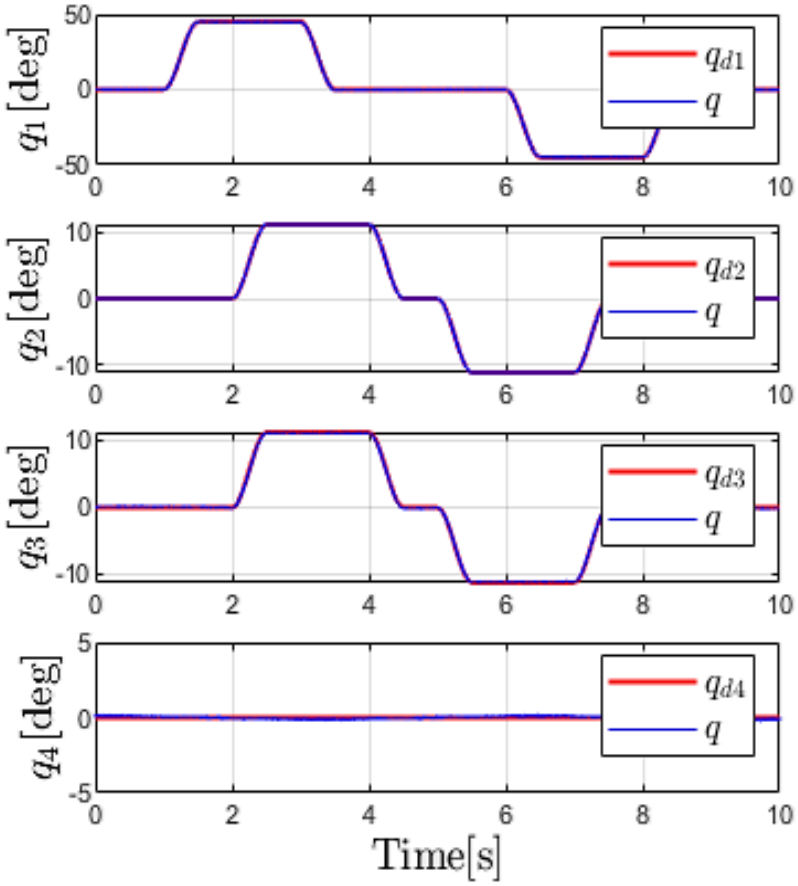

Fig. 6. QArm joint tracking

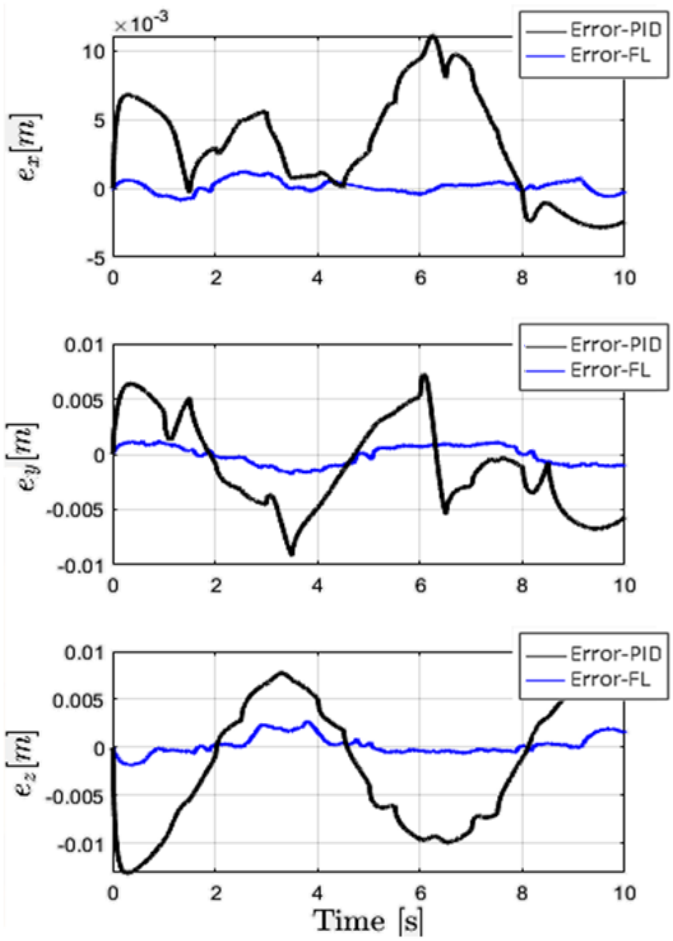

Fig. 7. Error in Feedback linearization and PID controllers

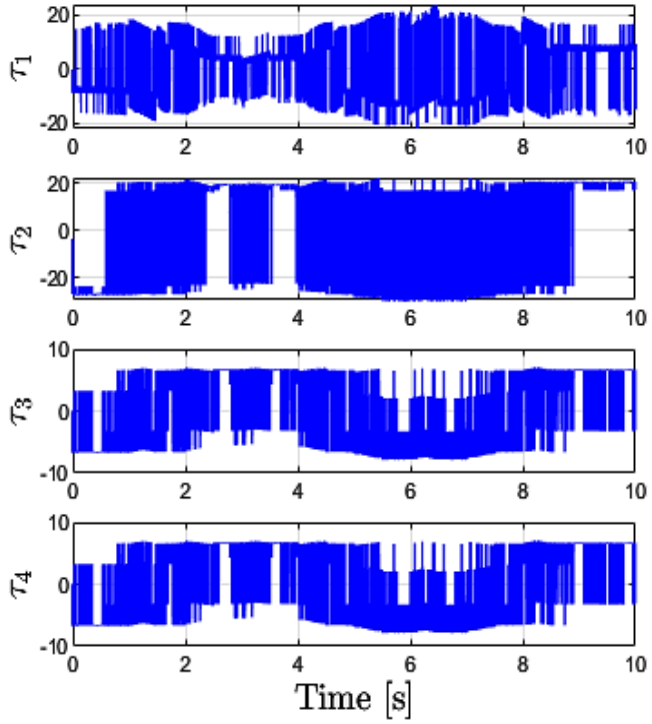

Fig. 8. Control signals

5. Conclusion

This paper presents a comprehensive approach to Feedback Linearization using a sliding mode tracking controller. The methodology leverages prior knowledge of the dynamic model, enabling the proposed controller to directly address the system's nonlinearity without the need for model linearization. By mitigating the effects of highly coupled dynamics, the controller ensures robust and precise tracking performance. The robustness characteristics are analyzed within the context of the global closed-loop system. Stability is examined through Lyapunov analysis, and the dynamic model is implemented in MATLAB/Simulink. The effectiveness of the proposed system is demonstrated through empirical results and a comparative analysis with a traditional PID controller, showcasing commendable performance and accuracy. Future research directions include comparing the proposed system with feedback linearization approaches based on alternative control systems to identify the most effective method. Future research can explore the following directions to enhance and extend the findings of this study such as Real-World Experimental Validation, Extension to Multi-Input Multi-Output (MIMO) Systems, Integration with Machine Learning Techniques, and Energy Efficiency and Computational Optimization.

Author Contribution: All authors contributed equally to the main contributor to this paper. All authors read and approved the final paper.

Funding: This research received no external funding.

Conflicts of Interest: The authors declare no conflict of interest.

References

[1] W. K. A. Alqaisi, "Nonlinear control and perturbation compensation in UAV quadrotor," *Thèse de doctorat électronique*, pp. 167-178, 2019, https://espace.etsmtl.ca/id/eprint/2372.

[2] H. Z. Ting, Han, M. H. M. Zaman, M. F. Ibrahim, and A. M Moubark, "Kinematic Analysis for Trajectory Planning of Open-Source 4-DoF Robot Arm," *International Journal of Advanced Computer Science and Applications (IJACSA)*, vol. 12, no. 6, pp. 768-775, 2021, https://dx.doi.org/10.14569/IJACSA.2021.0120690.

[3] Y. Kali, J. Rodas, M. Saad, R. Gregor, W. Alqaisi, and K. Benjelloun, "Robust Finite-time Position and Attitude Tracking of a Quadrotor UAV using Super-Twisting Control Algorithm with Linear Correction Terms," *Proceedings of the 16th International Conference on Informatics in Control, Automation and Robotics*, vol. 2, pp. 221–228, 2019, https://doi.org/10.5220/0007831202210228.

[4] M. Plooij, W. Wolfslag, and M. Wisse, "Robust feedforward control of robotic arms with friction model uncertainty," *Robotics and Autonomous Systems*, vol. 70, pp. 83–91, 2015, https://doi.org/10.1016/j.robot.2015.03.008.

[5] Q. Guo, T. Yu, and D. Jiang, "Robust H∞ positional control of 2-DOF robotic arm driven by electro-hydraulic servo system," *ISA Transactions*, vol. 59, pp. 55–64, 2015, https://doi.org/10.1016/j.isatra.2015.09.014.

[6] Z. Liu, C. Chen, Y. Zhang, and C. P. Chen, "Coordinated fuzzy control of robotic arms with actuator nonlinearities and motion constraints," *Information Sciences*, vol. 296, pp. 1–13, 2015, https://doi.org/10.1016/j.ins.2014.10.061.

[7] C. -C. Chen and Y. -T. Chen, "Feedback Linearized Optimal Control Design for Quadrotor With Multi-Performances," *IEEE Access*, vol. 9, pp. 26674-26695, 2021, https://doi.org/10.1109/ACCESS.2021.3057378.

[8] F. R. Al-Ani, O. F. Lutfy, and H. Al-Khazraji, "Optimal Synergetic and Feedback Linearization Controllers Design for Magnetic Levitation Systems: A Comparative Study," *Journal of Robotics and Control (JRC)*, vol. 6, no. 1, no. 1, pp. 22-30, 2024, https://doi.org/10.18196/jrc.v6i1.24452.

[9] A. Chemori, R. Kouki, and F. Bouani, "A new fast nonlinear model predictive control of parallel manipulators: Design and experiments," *Control Engineering Practice*, vol. 130, p. 105367, 2023, https://doi.org/10.1016/j.conengprac.2022.105367.

[10] A. Duka, "Neural network based inverse kinematics solution for trajectory tracking of a robotic arm," *Procedia Technology*, vol. 12, pp. 20–27, 2014, https://doi.org/10.1016/j.protcy.2013.12.451.

[11] W. Alqaisi and C. Z. El-Bayeh, "Backstepping Control Based on Neural Network Estimation," *Innovation and Technological Advances for Sustainability*, 2024, https://www.taylorfrancis.com/chapters/oa-edit/10.1201/9781003496724-24/backstepping-control-based-neural-network-estimation-walid-alqaisi-claude-ziad-el-bayeh.

[12] X. Yang *et al*., "Hierarchical Reinforcement Learning With Universal Policies for Multistep Robotic Manipulation," *IEEE Transactions on Neural Networks and Learning Systems*, vol. 33, no. 9, pp. 4727-4741, 2022, https://doi.org/10.1109/TNNLS.2021.3059912.

[13] T. Uzunovic, E. A. Baran, E. Golubovic, and A. Sabanovic, "A novel hybrid contouring control method for 3-DOF robotic manipulators," *Mechatronics*, vol. 40, pp. 178–193, 2016, https://doi.org/10.1016/j.mechatronics.2016.10.001.

[14] D. Verscheure, B. Demeulenaere, J. Swevers, J. De Schutter, and M. Diehl, "Practical time-optimal trajectory planning for robots: a convex optimization approach," IEEE Transactions on Automatic Control, pp. 1-10, 2008, https://lirias.kuleuven.be/bitstream/123456789/211749/1/07-208.pdf.

[15] C. -Y. Kai and A. -C. Huang, "Adaptive LQ control of robot manipulators," *2014 9th IEEE Conference on Industrial Electronics and Applications*, pp. 770-774, 2014, https://doi.org/10.1109/ICIEA.2014.6931266.

[16] K. Chen, "Robust optimal adaptive sliding mode control with the disturbance observer for a manipulator robot system," *International Journal of Control, Automation and Systems*, vol. 16, no. 4, pp. 1701–1715, 2018, https://doi.org/10.1007/s12555-017-0710-1.

[17] A. Perrusquía, "Robust state/output feedback linearization of direct drive robot manipulators: A controllability and observability analysis," *European Journal of Control*, vol. 64, p. 100612, 2022, https://doi.org/10.1016/j.ejcon.2021.12.007.

[18] J. Wilson, M. Charest, and R. Dubay, "Non-linear model predictive control schemes with application on a 2 link vertical robot manipulator," *Robotics and Computer-Integrated Manufacturing*, vol. 41, pp. 23–30, 2016, https://doi.org/10.1016/j.rcim.2016.02.003.

[19] W. Alqaisi and C. Z. El-Bayeh, "Adaptive Control Based on Radial Base Function Neural Network Approximation for Quadrotor," *2022 17th Annual System of Systems Engineering Conference (SOSE)*, pp. 214-219, 2022, https://doi.org/10.1109/SOSE55472.2022.9812660.

[20] T. Rybus, K. Seweryn, and J. Z. Sasiadek, "Control system for free-floating space manipulator based on nonlinear model predictive control (NMPC)," *Journal of Intelligent & Robotic Systems*, vol. 85, pp. 491–509, 2017, https://doi.org/10.1007/s10846-016-0396-2.

[21] W. Alqaisi, B. Brahmi, J. Ghommam, M. Saad, and V. Nerguizian, "Vision-based leader-follower approach for uncertain quadrotor dynamics using feedback linearisation sliding mode control," *International Journal of Modelling, Identification and Control*, vol. 33, no. 1, pp. 9-19, 2019, https://doi.org/10.1504/IJMIC.2019.103980.

[22] W. Alqaisi, B. Brahmi, J. Ghommam, M. Saad and V. Nerguizian, "Multivariable Super-Twisting Control in a Vision-based Quadrotor Utilized in Agricultural Application," *2018 IEEE International Conference on Computational Intelligence and Virtual Environments for Measurement Systems and Applications (CIVEMSA)*, pp. 1-6, 2018, https://doi.org/10.1109/CIVEMSA.2018.8439964.

[23] W. Alqaisi, Y. Kali and W. Lucia, "Finite-Time Flight Control of Uncertain Quadrotor UAV based on Modified Non-Singular Fast Terminal Super-Twisting Control," *2020 IEEE Conference on Control Technology and Applications (CCTA)*, pp. 37-42, 2020, https://doi.org/10.1109/CCTA41146.2020.9206250.

[24] W. Alqaisi, B. Brahmi, J. Ghommam, M. Saad and V. Nerguizian, "Sliding Mode Controller and Hierarchical Perturbation Compensator in a UAV Quadrotor," *2018 IEEE International Conference on*

Computational Intelligence and Virtual Environments for Measurement Systems and Applications (CIVEMSA), pp. 1-6, 2018, https://doi.org/10.1109/CIVEMSA.2018.8440003.

[25] A. Perrusquía, "Robust state/output feedback linearization of direct drive robot manipulators: A controllability and observability analysis," *European Journal of Control*, vol. 64, p. 100612, 2022, https://doi.org/10.1016/j.ejcon.2021.12.007.

[26] A. Elmogy and W. Elawady, "An adaptive continuous sliding mode feedback linearization task space control for robot manipulators," *Ain Shams Engineering Journal*, vol. 15, no. 1, p. 102284, 2024, https://doi.org/10.1016/j.asej.2023.102284.

[27] Y. Kali, M. Saad, and K. Benjelloun, "Nonsingular fast terminal second-order sliding mode for robotic manipulators based on feedback linearization," *International Journal of Dynamics and Control*, vol. 10, no. 1, pp. 296–305, 2022, https://doi.org/10.1007/s40435-021-00810-7.

[28] W. Alqaisi, Y. Kali and C. Z. El-Bayeh, "Modified Fast Terminal Super-Twisting Control for Uncertain Robot Manipulators," *2021 18th International Multi-Conference on Systems, Signals & Devices (SSD)*, pp. 1142-1147, 2021, https://doi.org/10.1109/SSD52085.2021.9429461.

[29] W. Alqaisi, B. Brahmi, J. Ghommam, M. Saad, and V. Nerguizian, "Hierarchical perturbation compensation system with ERL sliding mode controller in a quadrotor," *IFAC Journal of Systems and Control*, vol. 26, p. 100232, 2023, https://doi.org/10.1016/j.ifacsc.2023.100232.

[30] X. Yu, Y. Feng and Z. Man, "Terminal Sliding Mode Control – An Overview," *IEEE Open Journal of the Industrial Electronics Society*, vol. 2, pp. 36-52, 2021, https://doi.org/10.1109/OJIES.2020.3040412.

[31] S. Ding, J. H. Park, and C. Chen, "Second-order sliding mode controller design with output constraint," *Automatica*, vol. 112, p. 108704, 2020, https://doi.org/10.1016/j.automatica.2019.108704.

[32] J. Baek, M. Jin and S. Han, "A New Adaptive Sliding-Mode Control Scheme for Application to Robot Manipulators," *IEEE Transactions on Industrial Electronics*, vol. 63, no. 6, pp. 3628-3637, 2016, https://doi.org/10.1109/TIE.2016.2522386.

[33] A. Lozynskyy, L. Kasha, S. Pakizh, R. Sadovskyi, "Synthesis of PI- and PID-Regulators in Control Systems Derived by the Feedback Linearization Method," *Energy Engineering and Control Systems*, vol. 10, no. 2, pp. 120–130, 2024, https://doi.org/10.23939/jeecs2024.02.120.

[34] P. P. Bhangale, S. K. Saha, and V. P. Agrawal, "A dynamic model based robot arm selection criterion," *Multibody System Dynamics*, vol. 12, pp. 95-115, 2004, https://doi.org/10.1023/B:MUBO.0000044363.57485.39.

[35] A. A. Mohammed and M. Sunar, "Kinematics modeling of a 4-DOF robotic arm," *2015 International Conference on Control, Automation and Robotics*, pp. 87-91, 2015, https://doi.org/10.1109/ICCAR.2015.7166008.

[36] S. A. Chander, A. Mukherjee, V. D. Shivling, A. Singla, "Enhanced Euler–Lagrange Formulation for Analyzing Human Gait With Moving Base Reference," *Journal of Mechanisms and Robotics*, vol. 17, no. 1, p. 011006, 2025, https://doi.org/10.1115/1.4065520.

[37] G. D'Antuono, K. Y. Pettersen, L. R. Buonocore, J. T. Gravdahl, and M. D. Castro, "Dynamic model of a tendon-actuated snake robot using the Newton-Euler formulation," *IFAC-PapersOnLine*, vol. 56, no. 2, pp. 11639–11644, 2023, https://doi.org/10.1016/j.ifacol.2023.10.502.

[38] C. -H. Yu, "Experimental Implementation of Quantum Algorithm for Association Rules Mining," *IEEE Journal on Emerging and Selected Topics in Circuits and Systems*, vol. 12, no. 3, pp. 676-684, 2022, https://doi.org/10.1109/JETCAS.2022.3201097.

[39] Q. -Y. Fan, D. Wang and B. Xu, "H∞ Codesign for Uncertain Nonlinear Control Systems Based on Policy Iteration Method," *IEEE Transactions on Cybernetics*, vol. 52, no. 10, pp. 10101-10110, 2022, https://doi.org/10.1109/TCYB.2021.3065995.

[40] R. M. Berger and H. A. ElMaraghy, "Feedback linearization control of flexible joint robots," *Robotics and Computer-Integrated Manufacturing*, vol. 9, no. 3, pp. 239–246, 1992, https://doi.org/10.1016/0736-5845(92)90028-5.